Journal of Optometry (2017) 10, 63–68

Journal of Optometry

www.journalofoptometry.org

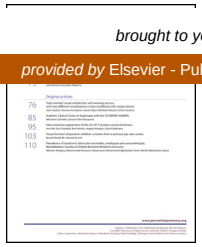

ORIGINAL ARTICLE

Influence of macular pigment optical density spatial distribution on intraocular scatter

Christopher M. Putnam*, Pauline J. Bland, Carl J. Bassi

University of Missouri-St Louis, College of Optometry, United States

Received 5 July 2015; accepted 22 September 2015
Available online 24 November 2015

KEYWORDS
Macular pigment optical density;
Spatial distribution;
Intraocular scatter

Abstract
Purpose: This study evaluated the summed measures of macular pigment optical density (MPOD) spatial distribution and their effects on intraocular scatter using a commercially available device (C-Quant, Oculus, USA).
Methods: A customized heterochromatic flicker photometer (cHFP) device was used to measure MPOD spatial distribution across the central 16° using a 1° stimulus. MPOD was calculated as a discrete measure and summed measures across the central 1°, 3.3°, 10° and 16° diameters. Intraocular scatter was determined as a mean of 5 trials in which reliability and repeatability measures were met using the C-Quant. MPOD spatial distribution maps were constructed and the effects of both discrete and summed values on intraocular scatter were examined.
Results: Spatial mapping identified mean values for discrete MPOD [0.32 (s.d. = 0.08)], MPOD summed across central 1° [0.37 (s.d. = 0.11)], MPOD summed across central 3.3° [0.85 (s.d. = 0.20)], MPOD summed across central 10° [1.60 (s.d. = 0.35)] and MPOD summed across central 16° [1.78 (s.d. = 0.39)]. Mean intraocular scatter was 0.83 (s.d. = 0.16) log units. While there were consistent trends for an inverse relationship between MPOD and scatter, these relationships were not statistically significant. Correlations between the highest and lowest quartiles of MPOD within the central 1° were near significance.
Conclusions: While there was an overall trend of decreased intraocular forward scatter with increased MPOD consistent with selective short wavelength visible light attenuation, neither discrete nor summed values of MPOD significantly influence intraocular scatter as measured by the C-Quant device.

* Corresponding author at: UMSL College of Optometry, 417 Marillac Hall, 1 University Blvd, St Louis, MO 63121-4400, United States.
E-mail address: cmpyv6@umsl.edu (C.M. Putnam).

http://dx.doi.org/10.1016/j.optom.2015.10.001

PALABRAS CLAVE
Densidad óptica del pigmento macular;
Distribución espacial;
Dispersión intraocular

Influencia de la distribución espacial de la densidad óptica del pigmento macular sobre la dispersión intraocular

Resumen
Objetivo: Este estudio evaluó la suma de las mediciones de la distribución espacial de la densidad óptica del pigmento macular (MPOD) y sus efectos sobre la dispersión intraocular, utilizando un dispositivo comercialmente disponible (C-Quant, Oculus, EEUU).
Métodos: Se utilizó un fotómetro intermitente heterocromático personalizado (cHFP) para medir la distribución espacial de la MPOD a lo largo de los 16° centrales, utilizando un estímulo de 1°. La MPOD se calculó como medición discreta y como las sumas de las mediciones a lo largo de los diámetros centrales de 1°, 3,3°, 10° y 16°. Se calculó la dispersión intraocular como media de los cinco ensayos en los que se lograron mediciones de fiabilidad y repetibilidad utilizando el dispositivo C-Quant. Se construyeron mapas de distribución espacial de la MPOD, examinándose los efectos sobre la dispersión intraocular, tanto de los valores discretos como de la suma de valores.
Resultados: El mapeado espacial identificó valores medios para la MPOD discreta [0,32 (DE = 0,08)], la suma de MPOD a lo largo de 1° central [0,37 (DE = 0,11)], la suma de MPOD a lo largo de 3,3° centrales [0,85 (DE = 0.20)], la suma de MPOD a lo largo de 10° centrales [1,60 (DE = 0,35)] y la suma de MPOD a lo largo de 16° centrales [1,78 (DE = 0,39)]. La dispersión intraocular media fue de 0,83 (DE = 0,16) unidades log. A pesar de producirse una tendencia consistente hacia una relación inversa entre MPOD y dispersión, dichas relaciones no fueron estadísticamente significativas. Las correlaciones entre los cuartiles superior e inferior de la MPOD dentro de 1° central fueron próximas a la significación estadística.
Conclusiones: A pesar de producirse una tendencia general hacia la disminución de la dispersión intraocular con el incremento de la MPOD, consistente con una atenuación selectiva de la luz visible con longitud de onda corta, ni los valores discretos ni la suma de valores de la MPOD reflejaron una influencia significativa sobre la dispersión intraocular, según las mediciones realizadas con el dispositivo C-Quant.

Introduction

van den Berg proposed a psychophysical method, termed direct compensation, to measure retinal light scatter in human observers.[1] Using this method, retinal light scatter was found to increase with age,[2] decrease with eye pigmentation,[3] and be related to a number of diseases.[4,5] While this technique was mainly used in the laboratory, a version that was simpler to understand, fast and criterion-independent was developed called the compensation comparison technique.[6] This device was subsequently developed for clinical use (C-Quant, Oculus Optikgeräte, Wetzler, Germany). The C-Quant gives reliable measures[6,7] and has been evaluated in subjects with cataracts,[8] contact lens wearers[9] and those undergoing refractive surgery patients.[10]

Retinal straylight has been shown to result in disability glare.[1,11,12] A number of studies have found that greater levels of macular pigment optical density (MPOD) are associated to a decrease in disability glare.[13–15] It seems reasonable to hypothesize that intraocular light scatter and MPOD may also be related.

However, two recent studies incorporating the C-Quant device demonstrated non-significant relationships between MPOD and intraocular scatter.[16,17] Several reasons have been proposed for this lack of association. Jongenelen et al.[16] included older subjects that may have influenced intraocular scatter values secondary to ocular transmission changes that occur with age. Jongenelen et al. further suggested the lack of correlation may result because macular pigment has peak absorption of short wavelengths and the C-quant uses an ''achromatic light source''. Beirne et al. also described the stimulus as being ''non-blue light dominant''.[17] Finally, another possible explanation is that both the Jongenelen et al. and Beirne study designs used only discrete MPOD measurements in their analyses while the C-Quant glare annulus has a 10° size. Thus, differences in the density of macular pigment outside the fovea may have an impact as well.

This study utilizes MPOD spatial mapping across the entire macula in a young cohort allowing summed measures of MPOD across central 1°, MPOD across 3.3° to match the C-Quant fixation target,[18] MPOD across 10° to match the C-Quant glare source outer diameter and MPOD across 16° to match the area of highest MP deposition within the retina. We also used a spectrophotometer for spectral analysis of the C-Quant glare source to determine the peak wavelength and spectral composition.

Methods

The current study included a total of 33 subjects derived from an *a priori* power analysis using an 80% power estimate and a Cohen's effect size of 0.5 expressed by the equation:

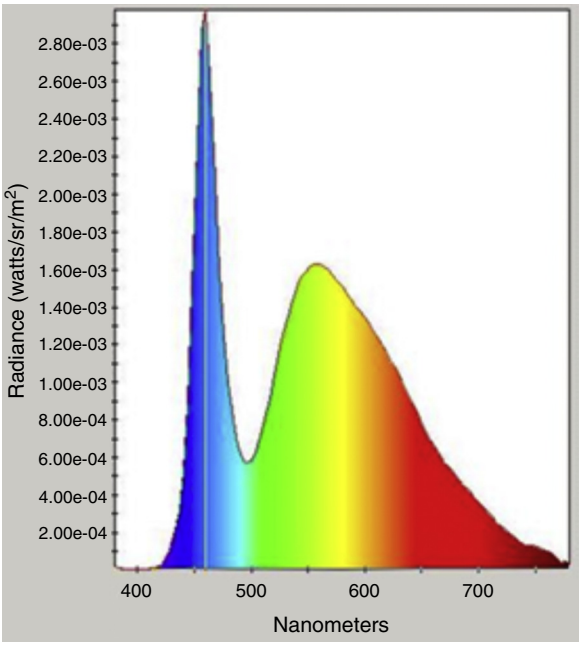

Figure 1 Spectral output of Oculus C-Quant glare source as measured with SpectraScan PR-650 (Photoresearch, CA).

$N = (2.8/0.5)^2 + 1$. Subjects performed all testing over a 4 week period.

Study inclusion criteria required no evidence of ocular pathology and best corrected visual acuity of 20/25 in the right eye and age less than 35 in order to avoid any presbyopic effects. Volunteer subjects were recruited from current optometry students enrolled at UMSL College of Optometry and were familiar with the devices and techniques presented during testing. The study sample included 11 males and 22 females with a mean age of 24.2 years (standard deviation [s.d.] = 2.7) and a range of 22–34 years. A detailed method of the cHFP spatial mapping of MPOD distribution is described by Putnam and Bassi.[19] The use of human subjects in this study was approved by the University of Missouri – St. Louis Institutional Review Board and adhered to the Declaration of Helsinki.

Intraocular forward scatter was assessed through a compensation comparison method using the C-Quant device (Oculus, USA). The C-Quant device is a commercially available clinical device able to measure forward scattered intraocular light through a comparison method. The C-Quant User Guide Technical Data indicates that the light source is a typical biphasic white LED. Spectral analysis of the C-Quant device was performed using a spectrophotometer (model 650; Photo Research Inc., Chatsworth, CA). The resulting spectral characteristics of the glare source indicated a white LED pattern with a peak wavelength output of 460 nm which coincides with the peak absorption of MP (Fig. 1).

The device uses hemifield comparison of flicker in which one side of the hemifield acts as the test field controlled by the subject and the other side acts as a fixed reference field. The flicker compensation is calculated using a 3.3° diameter target in conjunction with a glare source annulus with an inner diameter of 5° and an outer diameter of 10° and a background luminance of 25 cd/m^2. A 2AFC method is employed using a fixed temporal rate of 8 Hz assigned to one side of the hemifield. The subject is instructed to indicate the side of the hemifield in which flicker is perceived by using a right or left button. Intraocular scatter is assessed with the flicker rate between the two hemifields is perceived as equivalent. A complete description of the psychophysical technique is provided by van den Berg et al.[18] The validity and reliability algorithms are incorporated within the C-Quant device and all assessments of intraocular scatter followed the established guidelines of the commercial device. A mean intraocular scatter value was determined using the first 5 valid, repeatable measures as determined by the commercial device and represented as *ESD* and *Q* parameters. The *ESD* parameter is the standard deviation of the individual measured points and the *Q* parameter is the reliability coefficient. Intraocular scatter values that were included in the analysis had an *ESD* of ≤ 0.08 and a $Q \geq 1$.

The study utilized a novel device based on Wooten et al. that used customized heterochromatic flicker photometry (cHFP) to create a spatial distribution of MP across the central 16° of the retina.[20] The device was designed to create a spatial map of MPOD along four radii (0°, 90°, 180°, 270°) at 0°, 2°, 4°, 6°, and 8° eccentricities. This radial pattern was used to generate a spatial profile of an individual subject's MPOD. For a complete description, see Putnam et al.[19] The mean MPOD spatial distribution results along single radii for the 33 subject sample was fit to a 1st-order exponential decay curve to assess the variability in the data described by the r^2 value. Resulting MPOD spatial distribution profiles for each subject were also fit to a Lorentzian distribution curve using measured eccentricities along the entire 16° horizontal meridian. Using each subject's calculated Lorentzian distribution curve, summed MPOD values were calculated across the central 1° diameter, central 3.3° diameter, central 10° diameter and central 16° diameter of retina for each of the 33 subjects using OriginPro9 software (OriginPro Corp, Northampton, MA). The example below depicts a 1° diameter summed region within a Lorentzian distribution (Fig. 2).

Mean intraocular scatter was correlated with the five separate measures of MPOD: (1) discrete MPOD measured with 1° stimulus, (2) MPOD summed across central 1°, (3) MPOD summed across central 3.3°, (4) MPOD summed across central 10° and (5) MPOD summed across central 16°. These areas correspond to the macular pigment levels derived from previous studies,[16,17] total estimated MPOD from stimulus area, total estimated MPOD from the C-Quant target area, total estimated MPOD from the C-Quant glare source area, and total estimated MPOD across the entire macula.

Results

Macular pigment spatial distribution

The cHFP device identified reliable MPOD spatial distribution maps and showed a 1st order exponential decay function with eccentricity along single radii with a $r^2 = 0.912$ across the 33 subject study sample as previously reported by Putnam and Bassi.[15] The resulting MPOD values at each retinal eccentricity are a mean of the superior inferior, nasal and temporal measurements from all 33 subjects. Standard error of the mean measured for 0° eccentricity was less than

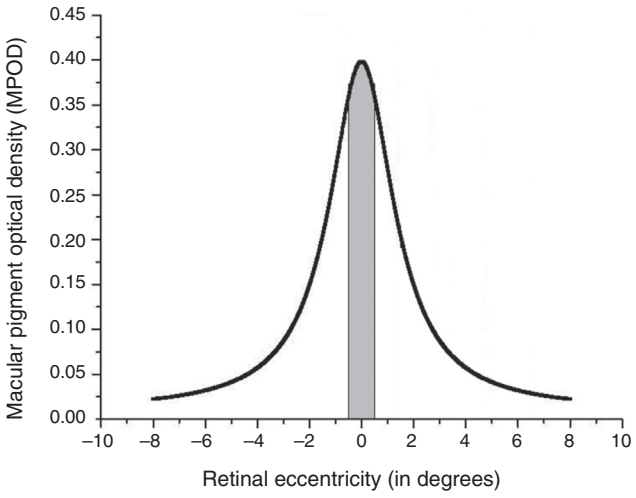

Figure 2 An example of the summation calculation performed across the 1° stimulus diameter for each subject. The 3.3°, 10° and 16° summation values were calculated in the same way, centered at 0° with an increasing diameter. The ordinate represents measured MPOD and the abscissa represents retinal eccentricity relative to the foveal center at 0°. The negative values along the abscissa were used in the OriginPro9 program to allow summation under a continuous curve extending 16° across the macula. The figure depicts MPOD spatial distribution extending form 8° nasal eccentricity (abscissa = −8) to 8° temporal eccentricity (abscissa = 8).

0.01 log unit, 2° eccentricity was 0.01, 4° eccentricity was 0.01 and 6° eccentricity was 0.02 log unit. Mean MPOD values for the 33 subject sample were 0.32 (s.d. = 0.08) for MPOD measured as discrete point, 0.37 (s.d. = 0.11) for MPOD summed across 1°, 0.85 (s.d. = 0.20) for MPOD summed across 3.3°, 1.60 (s.d. = 0.35) for MPOD summed across 10° and 1.78 (s.d. = 0.39) for MPOD summed across central16° (Table 1).

Intraocular scatter correlations with MPOD

The mean straylight value for the 33 subject sample was 0.83 (s.d. = 0.16), with a range of 0.61–1.38. While an inverse relationship was found between intraocular scatter and all MPOD measurements, none of these were found to be significant: intraocular scatter correlations with discrete MPOD ($r = -0.311$, $p = 0.078$), summed MPOD across central 1° ($r = -0.305$, $p = 0.084$), summed MPOD across central 3.3° ($r = -0.296$, $p = 0.095$), summed MPOD across central 10° ($r = -0.260$, $p = 0.145$) and summed MPOD across central 16° ($r = -0.261$, $p = 0.142$) (Table 2).

Discrete MPOD measures demonstrated the highest correlation with intraocular scatter. An independent Sample *t*-test analysis of intraocular scatter differences between the highest and lowest quartiles of foveal MPOD found a difference near significance ($t = -2.099$, $p = 0.054$). A scatterplot of discrete MPOD and intraocular scatter for all 33 subjects demonstrated a negative linear regression (Fig. 3).

Discussion

Intraocular scatter correlations with both discrete and summed MPOD measurements were non-significant. However, quartile analysis of the highest and lowest central 1° MPOD found near significant differences in intraocular scatter values consistent with previous findings.[16,17] The spectral composition of the glare annulus contained a large SW light component with a peak wavelength of 460 nm closely matching the spectral absorption characteristics of MP.

Several important differences between our study and existing literature can be found. First, previous studies of intraocular scatter have utilized only discrete MPOD measurements. Given that the C-Quant device (Oculus, USA) utilizes a 3.3° diameter flickering target in conjunction with a glare source annulus with an inner radius of 5° and an

Table 1 Mean MPOD values for the 33 subject sample measured as a MPOD discrete value, MPOD summed across central 1°, MPOD summed across central 3.3°, MPOD summed across central10° and MPOD summed across central 16°.

	MPOD discrete point	MPOD summed across 1°	MPOD summed across 3.3°	MPOD summed across 10°	MPOD summed across 16°
Mean	0.32	0.37	0.85	1.60	1.78
Std Dev	0.08	0.11	0.20	0.35	0.39

Table 2 Correlation coefficients for intraocular scatter thresholds and MPOD measured as a discrete value, MPOD summed across central 1°, MPOD summed across central 3.3°, MPOD summed across central 10° and MPOD summed across central 16°.

	MPOD discrete point	MPOD summed across 1°	MPOD summed across 3.3°	MPOD summed across 10°	MPOD summed across 16°
Intraocular scatter					
Pearson correlation	−0.311	−0.305	−0.296	−0.260	−0.261
Sig. (2-tailed)	0.078	0.084	0.095	0.145	0.142

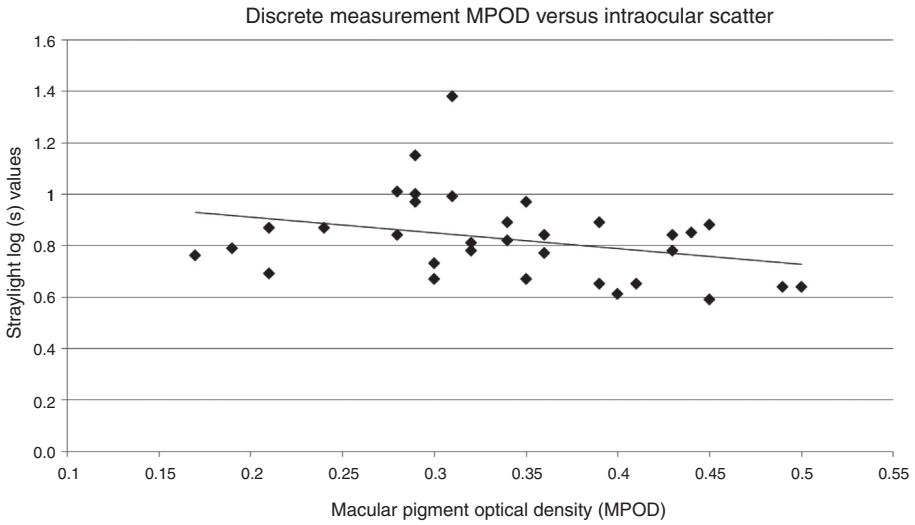

Figure 3 Scatterplot of discrete measurement MPOD *versus* intraocular scatter. The resulting linear regression fit equation was $y = -0.612x + 1.035$ with a covariance value of $r^2 = 0.097$.

outer radius of 10°, the effect of MP spatial distribution across the central 16° is relevant. Secondly, direct measurement of the glare source using a spectrophotometer (Photo Research, model 650) demonstrated a strong SW component inconsistent with Beirne's hypothesis.[17] Third, previous studies evaluating the relationship between discrete MPOD and intraocular scatter have utilized subjects with greater mean age, larger age range and subjects over 35 years of age.[16,21]

We were unable to replicate the significant negative correlation between intraocular scatter and MPOD identified by Puell et al.[21] Our findings agree with previous literature that failed to find a significant correlation between discrete MPOD and intraocular scatter. Interestingly, even with differences in experimental design, our data follows the same general inverse trend between both discrete and summed MPOD with intraocular scatter as the Jongenelen et al. and the Beirne studies.[16,17]

Intraocular scatter is highly influenced by inhomogeneities within the ocular media, lens transmission being a primary source. The finding of a non-significant correlation between MPOD and intraocular scatter values may be a result of the potential range of ocular transmission values. Further study on the influences of L and Z supplementation on resulting intraocular scatter values in healthy, younger subjects may be warranted.

Conflicts of interest

The authors have no conflicts of interest to declare.

Acknowledgements

The authors want to thank Wayne Garver and Michael Howe for their engineering and mechanical expertise during the development of the UMSL heterochromatic flicker photometer and to Oculus, USA, for the generous loan of the C-Quant device.

References

1. van den Berg TJ. Importance of pathological intraocular light scatter for visual disability. *Doc Ophthalmol*. 1986;61:327–333.
2. van den Berg TJ. Analysis of intraocular straylight, especially in relation to age. *Optom Vis Sci*. 1995;72:52–59.
3. van den Berg TJ. Dependence of intraocular straylight on pigmentations and light transmission through the ocular wall. *Vis Res*. 1991;31:1361–1367.
4. De Waard PW, Ljspeert JK, van den Berg TJ, de Jong PT. Intraocular light scattering in age-related cataracts. *Invest Ophthalmol Vis Sci*. 1992;33:618–625.
5. van den Berg TJ. Red glasses and visual function in retinitis pigmentosa. *Doc Ophthalmol*. 1992;73:255–274.
6. Franssen L, Coppens JE, van den Berg JT. Comparison method for assessment of retinal straylight. *Invest Ophthalmol Vis Sci*. 2006;47:768–776.
7. Guber I, Bachman LM, Guber J, Bochman F, Lange AP, Thiel MA. Reproducibility of straylight measurement by C-Quant for assessment of retinal straylight using the compensation comparison method. *Grafes Arch Clin Exp Ophthalmol*. 2011;249:1367–1371.
8. van der Meulen IJ, Gjertsen J, Kruijt B, et al. Straylight measurements as an indication for cataract surgery. *J Cataract Refract Surg*. 2012;38:840–848.
9. van der Meulen IJ, Engelbrecht LA, van Vliet JM, et al. Straylight measurements in contact lens wear. *Cornea*. 2010;29:516–522.
10. Li J, Wang Y. Characteristics of straylight in normal young myopic eyes and changes before and after LASIK. *Invest Ophthalmol Vis Sci*. 2011;52:3069–3073.
11. Vos JJ. Disability glare-a state of the art report. *Com Int de L'Eclairage J*. 1984;3:39–53.
12. Elliot DB, Bullimore MB. Assess the reliability, discriminative ability, and validity of disability glare tests. *Invest Ophthalmol Vis Sci*. 1993;34:108–119.
13. Stringham JM, Hammond BR. Macular pigment and visual performance under glare conditions. *Optom Vis Sci*. 2008;85:82–88.
14. Stringham JM, Garcia PV, Smith PA, McLin LN, Foutch BK. Macular pigment and visual performance in glare: benefits for

photostress recovery, disability glare, and visual discomfort. *Invest Ophthalmol Vis Sci*. 2011;52:7406–7415.
15. Hammond BR, Wooten BR, Engles M, Wong JC. The influence of filtering by the macular carotenoids on contrast sensitivity measured under simulated blue haze conditions. *Vis Res*. 2012;63:58–62.
16. Jongenelen S, Rozema JJ, Tassignon MJ. Influence of macular pigment on retinal straylight in healthy eyes. *Invest Ophthalmol Vis Sci*. 2013;54:3505–3509.
17. Beirne RO. Macular pigment levels do not influence C-Quant retinal straylight estimates in young Caucasians. *Clin Exp Optom*. 2014;97:171–174.
18. van den Berg TJ, Franssen L, Kruijt B, Coppens JE. Psychophysics, reliability, and norm values for temporal contrast sensitivity implemented on the two alternative forced choice C-Quant device. *J Biomed Opt*. 2011;16:85004.
19. Putnam CM, Bassi CJ. Macular pigment spatial distribution effects on glare disability. *J Optom*. 2015;8:258–265.
20. Wooten BR, Hammond BR, Land RI, Snodderly DM. A practical method for measuring macular pigment optical density. *Invest Ophthalmol Vis Sci*. 1999;40:2481–2489.
21. Puell M, Perez-Carrasco MJ, Barrio A, Palomo-Alvarez C, Sanchez R. Relationship between macular pigment and straylight on the retina. *Acta Ophthalmol*. 2008;86:243.